

Impairment of Store-Operated Ca²⁺ Entry in TRPC4^{-/-} Mice Interferes With Increase in Lung Microvascular Permeability

Chinnaswamy Tiruppathi, Marc Freichel,* Stephen M. Vogel,* Biman C. Paria, Dolly Mehta, Veit Flockerzi, Asrar B. Malik

Abstract—We investigated the possibility that the TRPC gene family of putative store-operated Ca²⁺ entry channels contributes to the increase in microvascular endothelial permeability by prolonging the rise in intracellular Ca²⁺ signaling. Studies were made in wild-type (wt) and TRPC4 knockout (TRPC4^{-/-}) mice and lung vascular endothelial cells (LECs) isolated from these animals. RT-PCR showed expression of TRPC1, TRPC3, TRPC4, and TRPC6 mRNA in wt LECs, but TRPC4 mRNA expression was not detected in TRPC4^{-/-} LECs. We studied the response to thrombin because it is known to increase endothelial permeability by the activation of G protein-coupled proteinase-activated receptor-1 (PAR-1). In wt LECs, thrombin or PAR-1 agonist peptide (TFLLRNPNNDK-NH₂) resulted in a prolonged Ca²⁺ transient secondary to influx of Ca²⁺. Ca²⁺ influx activated by thrombin was blocked by La³⁺ (1 μmol/L). In TRPC4^{-/-} LECs, thrombin or TFLLRNPNNDK-NH₂ produced a similar initial increase of intracellular Ca²⁺ secondary to Ca²⁺ store depletion, but Ca²⁺ influx induced by these agonists was drastically reduced. The defect in Ca²⁺ influx in TRPC4^{-/-} endothelial cells was associated with lack of thrombin-induced actin-stress fiber formation and a reduced endothelial cell retraction response. In isolated-perfused mouse lungs, the PAR-1 agonist peptide increased microvessel filtration coefficient (K_{fc}), a measure of vascular permeability, by a factor of 2.8 in wt and 1.4 in TRPC4^{-/-}; La³⁺ (1 μmol/L) addition to wt lung perfusate reduced the agonist effect to that observed in TRPC4^{-/-}. These results show that TRPC4-dependent Ca²⁺ entry in mouse LECs is a key determinant of increased microvascular permeability. (*Circ Res.* 2002;91:70-76.)

Key Words: mouse lung endothelial cells ■ thrombin-induced Ca²⁺ influx ■ TRPC4 knockout
■ lung microvascular permeability

Endothelial cell activation induced by thrombin plays an important role in the pathogenesis of vascular injury and tissue inflammation.^{1,2} In lungs, thrombin increases vascular permeability and tissue water content.^{1,2} Thrombin mediates these effects by activation of G protein-coupled proteinase-activated receptor-1 (PAR-1) expressed on the endothelial cell surface. We have shown thrombin fails to increase lung microvascular permeability in PAR-1 null mice.³ Increase in intracellular Ca²⁺ signaling is critical in the mechanism of increased endothelial permeability after activation of PAR-1.⁴⁻⁷ Thrombin-induced increase in intracellular Ca²⁺ concentration in endothelial cells is dependent on both inositol 1,4,5-trisphosphate (IP₃)-induced release of stored Ca²⁺ and Ca²⁺ store depletion-mediated Ca²⁺ influx.⁵ We have shown recently that the prevention of Ca²⁺ influx in endothelial cells markedly reduced the thrombin-induced increase in permeability.^{5,6} The Ca²⁺ influx in this model required the activa-

tion of *Src* tyrosine kinase in endothelial cells.⁸ Ca²⁺ influx secondary to store depletion, the capacitative Ca²⁺ entry, is mediated by store-operated cation channels (SOCs).^{9,10} SOC channels can be activated by IP₃-induced store depletion and by inhibition of Ca²⁺-ATPase (SERCA) with agents such as thapsigargin, cyclopiazonic acid, or dibenzohydroquinone (BHQ).^{9,10}

Studies have identified the mammalian homologues of *Drosophila* transient receptor potential (TRP) gene family of channels expressed in the plasma membrane of cells that function as SOC channels.^{9,10} TRP genes encode a superfamily of proteins with 6 transmembrane helices, which can be divided into at least 3 subfamilies; ie, TRPC, TRPV, and TRPM.¹¹ Members of the TRPC protein subfamily contain 700 to 1000 amino acids and 7 isoforms (TRPC1 to 7) are expressed in mammalian cells.⁹ Members of the TRPC family are divalent cation selective and nonselective cation channels.^{9,10} They are

Original received January 16, 2002; revision received May 1, 2002; accepted May 15, 2002.

From the Department of Pharmacology, The University of Illinois, Chicago, Ill; and Universitat des Saarlandes (M.F., V.F.), Institut für Pharmakologie und Toxikologie, Homburg, Germany.

*Both authors contributed equally to this work.

Correspondence to Asrar B. Malik, PhD, Distinguished Professor and Head, Dept of Pharmacology M/C868, College of Medicine, University of Illinois at Chicago, 835 S Wolcott Ave, Chicago, IL 60612. E-mail abmalik@uic.edu

© 2002 American Heart Association, Inc.

Circulation Research is available at <http://www.circresaha.org>

DOI: 10.1161/01.RES.0000023391.40106.A8

activated by Ca²⁺ store depletion induced by the G_q-protein-phospholipase C system.^{9,10,12–15} Primary endothelial cells in culture express TRPC1, TRPC2, TRPC3, TRPC4, TRPC5, and TRPC6.^{9,10,15,16} Studies have demonstrated the expression of TRPC1, TRPC2, TRPC3, TRPC4, and TRPC6 gene mRNA in mouse aortic endothelial cells.^{10,17} Freichel et al¹⁷ investigated store-operated Ca²⁺ current and Ca²⁺ entry in aortic endothelial cells (AECs) derived from TRPC4 knock-out (TRPC4^{-/-}) mice. They showed that IP₃/BHQ-activated SOC current was absent in these AECs compared with wild-type (wt) AECs.¹⁷ Also, acetylcholine-induced endothelium-dependent smooth muscle relaxation was blunted in vessels lacking TRPC4 compared with wt. Because thrombin is a potent proinflammatory mediator and mediates increased endothelial permeability dependent on intracellular Ca²⁺ signaling, in the present study, we have investigated permeability response in the TRPC4^{-/-} mice. We show that Ca²⁺ entry in response to thrombin was drastically reduced in lung endothelial cells obtained from TRPC4^{-/-} mice. Further, the thrombin-induced increase in lung microvascular permeability was reduced 50% compared with controls. Thus, TRPC4-dependent Ca²⁺ entry is a critical determinant of the thrombin-induced increase in vascular endothelial permeability.

Materials and Methods

Materials

Human α -thrombin was obtained from Enzyme Research Laboratories (South Bend, Ind). PAR-1-specific agonist peptide (TFLLRNPNDK-NH₂) was synthesized as C-terminal amide at University of Illinois Protein Sciences Facility, Urbana, Ill. The peptide purity was greater than 95%. Endothelial Growth Medium (EGM-2) was obtained from Clonetics. Hanks' balanced salt solution (HBSS), L-glutamine, phosphate buffered saline (PBS), and trypsin were obtained from Life Technologies, Inc. Fetal bovine serum (FBS) was obtained from Hyclone Laboratories, Inc. Fura 2-AM was purchased from Molecular Probes.

Targeted Disruption of TRPC4 Gene in Mice

TRPC4 gene was disrupted in mice as described by Freichel et al¹⁷ using the homologous recombination method. TRPC4 transcript expression was absent in these TRPC4^{-/-} mice. In the present study, the loss of TRPC4 mRNA was confirmed by RT-PCR (shown in Figure 1). TRPC4 transcript expression was detected in wt mice lung endothelial cells, but TRPC4 transcript expression was not detectable in TRPC4^{-/-} mice. For all studies wild-type 129SvJ or TRPC4^{-/-} mice that were backcrossed for 5 generations into 129SvJ genetic background were used.

Lung Endothelial Cell Isolation and Culture

According to an approved protocol of the University of Illinois Animal Care Committee, female 129SvJ (wild-type) or TRPC4^{-/-} mice weighing 30 to 35 g were anesthetized with 3% halothane, and heparin (50 U/mouse) was injected into the jugular vein. All animals used in this study were obtained from colonies located at the Institut für Pharmakologie Universität des Saarlandes, und Toxikologie, Homburg, Germany. The abdominal cavity was opened and the pulmonary artery was cannulated. Krebs-Henseleit solution supplemented with bovine serum albumin (5 g/100 mL) was infused to remove blood. Lungs were removed and placed inside a culture hood. Lung tissue slices from 3 mice were prepared, washed, and suspended in HBSS. Excess HBSS was aspirated, and the tissue slices were minced and transferred to a 15-mL sterile tube. The minced tissues were suspended in 10 mL of collagenase A (1.0

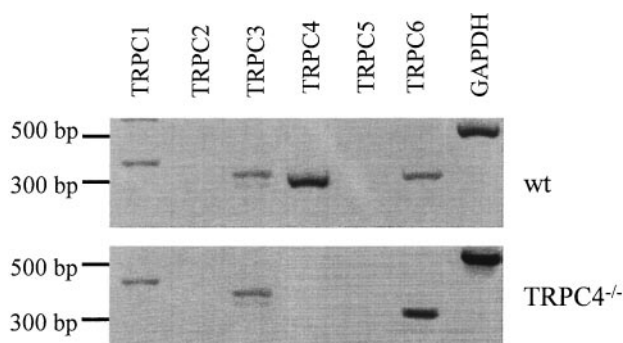


Figure 1. Expression profile of the TRPC subfamily gene transcripts in LECs from wt and TRPC4^{-/-} mice. Total RNA was first isolated from LECs, using Trizol Reagent (GIBCO/BRL), and then treated with DNase. Total RNA (2 μ g) was reverse-transcribed using a SuperScript preamplification kit (GIBCO/BRL). The following mouse gene specific primers were used for PCR¹⁰: mTRPC1, forward 5'-GATTTTGGGAA-ATTTCTGGG-3', reverse 5'-TGTTATCAGCTGGAAGT-3'; mTRPC2, forward 5'-GACATGATCCGGTTCATG-3', reverse 5'-CTGGATCTT-CTGGAAGGA-3'; mTRPC3, forward 5'-GACATATCAAGTTCATGGT-3', reverse 5'-CTGGATCTCTTGGTATGA-3'; mTRPC4, forward 5'-TGGGACATGTGGCACCCAC-3', reverse 5'-ACGTGGAAAACG-CGTTGTCTG-3'; mTRPC5, forward 5'-GACTAGTCTTGATATACT-CAAATTTCTC-3', reverse 5'-GGGGTACCTCAGCATGATGGCAA-TG-3'; mTRPC6, forward 5'-GATATCTTCAAATTCATGGTC-3', reverse 5'-CTCAATTTCTGGAATGAAC-3'; mGAPDH, forward 5'-G TGAAGGTCGGGTGAACGG-3', reverse 5'-TCATGAGCCCTTCCAC-AATG-3'. Expected length of amplified fragments were 356, 297, 309, 304, 365, 309, and 517 base pairs for mTRPC1, mTRPC2, mTRPC3, mTRPC4, mTRPC5, mTRPC6, and GAPDH, respectively. Note that mTRPC4 transcript expression was not detectable in LECs from TRPC4^{-/-} mice. RT-PCR profile was compared with housekeeping gene GAPDH. The experiment was repeated 3 times.

mg/mL in HBSS) and digested for 60 minutes at 37°C with gentle shaking. The released cells were centrifuged at 200g for 10 minutes. The pellet was suspended in 10 mL suspension buffer (Ca²⁺- and Mg²⁺-free PBS containing 0.5 g/100 mL bovine serum albumin, 2 mmol/L EDTA, and 4.5 mg/mL D-glucose), and filtered through 200- μ m mesh filter. The filtered cell suspension was centrifuged at 200g for 10 minutes and suspended in 10 mL of suspension buffer. To this cell suspension, 1.5 μ g/mL anti-mouse PECAM-1 antibody (BD Pharmingen) was added and incubated at 4°C for 30 minutes with gentle shaking. The cell suspension was centrifuged to remove unbound antibody and washed once with suspension buffer. The washed cells were incubated with Dynabeads M-450 (Sheep anti-rat IgG) for 30 minutes at 4°C. After this incubation period, the cell suspension was attached to a magnetic column and the unbound cells were aspirated. Cells bound to the magnetic beads were washed once with HBSS and digested with trypsin for 3 minutes at 22°C. The cells released from the magnetic beads were separated, washed, and suspended in growth medium (EGM-2 supplemented with 10% FBS). The cell suspension was plated on Matrigel (BD Bioscience)-coated 35-mm culture dish and allowed to grow to confluence for 10 days. Cells were then harvested from the Matrigel plates by dispase (BD Bioscience) for 60 to 90 minutes. Cells were washed after dispase treatment once with growth medium and plated on 0.1% gelatin coated culture dish. Cells passaged between 3 and 4 times were used in experiments. Endothelial cells were characterized by their cobblestone morphology, platelet/endothelial cell adhesion molecule-1 (PECAM-1 or CD31) expression, and Dil-Ac-LDL uptake.

Cytosolic Ca²⁺

Thrombin-induced increase in cytosolic Ca²⁺ ([Ca²⁺]_i) was measured using the Ca²⁺-sensitive fluorescent dye fura 2.¹⁸ Cells were grown to confluence on 0.1% gelatin-coated 22-mm glass cover slips and then washed 2 times with HBSS and loaded with fura 2-AM (5

$\mu\text{mol/L}$) for 1 hour at 37°C . After the loading, cells were washed twice with HBSS. Cells were imaged using an Attoflor Ratio Vision digital fluorescence microscopy system (Atto Instruments) equipped with a Zeiss Axiovert S100 inverted microscope and F-Fluar $40\times$, 1.3 NA oil immersion objective. Regions of interest in individual cells were marked and excited at 334 and 380 nm with emission at 520 nm at 5-second intervals. At the end of each experiment, ionomycin ($10 \mu\text{mol/L}$) was added to obtain fluorescence of Ca^{2+} -saturated fura 2 (high $[\text{Ca}^{2+}]_i$) and EGTA (10 mmol/L) to obtain fluorescence of free fura 2 (low $[\text{Ca}^{2+}]_i$). $[\text{Ca}^{2+}]_i$ was calculated based on a dissociation constant (K_d) of 225 nmol/L with a 2 point fit curve.

Transendothelial Cell Electrical Resistance

Thrombin-induced endothelial cell retractile response was measured as described.¹⁹ Briefly, endothelial cells were seeded on gelatin-coated gold electrodes ($5.0\times 10^{-4} \text{ cm}^2$) and grown to confluence. The small electrode and the larger counter electrode were connected to a phase-sensitive lock-in amplifier. Constant current $1 \mu\text{A}$ was supplied by a 1 V, 4000 Hz AC signal connected serially to 1 M Ω resistor between the small electrode and larger counter electrode. Voltage between small electrode and large electrode was monitored by lock-in amplifier, stored, and processed by a PC. The computer also controlled the output of the amplifier and switched the measurement to different electrodes in the course of each experiment. Before the experiment, confluent endothelial monolayer was kept in 1% FBS containing medium for 2 hours and then thrombin-induced change in resistance of endothelial monolayer was measured. Data are presented in resistance normalized to its value at time 0 as described.^{6,19}

Distribution of Actin Stress Fibers

Endothelial cells were grown to confluence on gelatin-coated glass cover slips. Cells were incubated with 1% FBS supplemented growth medium for 2 hours before exposure with thrombin (5 U/mL) for different time intervals. Cell were washed and fixed for 15 minutes with 2% paraformaldehyde in HBSS containing 10 mmol/L HEPES buffer (pH 7.4) at room temperature. Cells were thoroughly rinsed 3 times with HBSS, and then permeabilized with 0.1% Triton X-100 for 30 minutes. After rinsing, cells were incubated with 1% bovine serum albumin in HBSS followed by incubation with Alexa-488 labeled phalloidin plus DAPI to stain actin filaments and nuclei, respectively. Cells were then washed 3 times with HBSS, mounted with Prolong Antifade mounting medium and viewed with $60\times$ objective in Zeiss LSM 510 confocal microscope.

Perfused Mouse Lung Preparation

According to approved protocol of University of Illinois Animal Care Committee, male 129SvJ mice weighing 30 to 35 g were anesthetized using 2.5% halothane. Anesthesia was maintained with 1.5% halothane delivered through a nose cone. The trachea was cannulated with a stainless steel tube for constant positive pressure ventilation with the anesthetic gas mixture. Heparin (50 U) was injected into the right jugular vein to prevent blood clotting. A thoracotomy was performed to expose the heart and lungs. An incision was made in the right ventricle at the base of the pulmonary artery for introducing pulmonary arterial cannula. A polyethylene cannula (PE 60; Becton Dickinson) was advanced into the pulmonary artery and secured by a suture. For drainage of pulmonary venous effluent, a catheter (made of a 3-mm length of PE-50 tubing) was inserted through the left atrium and secured. The lung preparation was perfused in situ using a peristaltic pump. The anesthetic gas flow was terminated when perfusion was begun, and ventilation was continued with room air. The heart and the exsanguinated lungs were rapidly excised and transferred en bloc to a perfusion apparatus, where lung preparations were suspended from an electronic beam balance. The isolated lung preparations were ventilated at 186 breaths/min and end-expiratory pressure of $2 \text{ cm H}_2\text{O}$, and perfused at constant flow (2 mL/min), temperature (37°C), and venous pressure ($+1 \text{ cm H}_2\text{O}$) with a modified Krebs-Henseleit solution (composition in mmol/L : NaCl 118; KCl 4.7; CaCl_2 1.0; MgCl_2 0.5;

HEPES sodium 4.43; HEPES free acid 5.57; NaHCO_3 3; glucose 11; EDTA 0.025; pH 7.4) supplemented with 3.0 g/100 mL of bovine serum albumin (BSA, Fraction V, 99% pure and endotoxin-free; Sigma-Aldrich). Pulmonary arterial pressure was monitored using a Gould pressure transducer (Model P23ID; Gould Instruments Inc). Lung wet weight was electronically nulled when the tissue was mounted, and subsequent weight changes due to gain or loss of fluid from the lung were recorded. Lung weight and arterial pressure recordings were displayed on a computer video monitor with the aid of amplifiers (Model CP122; Astro-Med), an analog-to-digital converter ($\mu\text{CDAS-8PGA}$ board; Keithley Metrabyte), and commercial software for acquisition and logging of data (Notebook Pro for Windows; Labtech). All lung preparations underwent a 20-minute equilibration perfusion. Lung preparations were discarded if they were not isogravimetric at the end of the equilibration period.

Capillary Filtration Coefficient Measurement

Pulmonary capillary filtration coefficient (K_{fc}) was measured to determine microvascular permeability to liquid. Briefly, in the isogravimetric condition, outflow pressure was rapidly elevated by $+5 \text{ cm H}_2\text{O}$ for 4 minutes. The ensuing changes in lung wet weight reflect a rapid rise in vascular volume followed by a slower phase of net fluid extravasation. A double exponential function was fitted to the data (with the aid of a Lotus 1-2-3 macro); K_{fc} was calculated from initial slope of slower exponential component normalized to the outflow pressure change and to lung wet weight. Lung wet weight was calculated from the dry weight of the lung (determined at the conclusion of each experiment) multiplied by the wet:dry weight ratio as described.³ This ratio in 6 freshly isolated (nonperfused) mouse lungs was 6.04 ± 0.4 . Preliminary experiments in normal control mouse lung preparations determined that, in the same lung preparation, 3 successive measurements of K_{fc} separated by an interval of 20 minutes were identical.

Effects of PAR-1 Agonist Peptide on K_{fc}

In experiments testing the effects of PAR-1 agonist peptide on K_{fc} , the perfusion rate was reduced to 1.8 mL/min and perfusing liquid, containing either PAR 1 agonist peptide or no drug (baseline condition), was infused via a side-port at a rate of 0.2 mL/min . K_{fc} measurements were made at baseline, and after a 20-minute exposure to PAR-1 agonist peptide (TFLLRNPNKD-NH₂); in some preparations, a third K_{fc} measurement was made after a 20-minute drug washout period. The values are expressed as the ratio of experimental-to-basal K_{fc} values in the same lung preparation.

Statistical Analysis

Statistical comparisons were made using the 2-tailed Student's *t* test. Values are reported as mean \pm SEM. Values were considered significant at $P < 0.05$.

Results

Mouse Lung Endothelial Characterization and Validation of TRPC4^{-/-} Mice

We isolated LECs from wt and TRPC4^{-/-} mice. TRPC4 gene expression was absent in TRPC4^{-/-} mice (Figure 1). TRPC4 was markedly expressed in wt LECs compared with the other TRPC isoforms (Figure 1). TRPC2 and TRPC5 transcripts were not detectable, whereas TRPC1, TRPC3, and TRPC6 were expressed in wt and TRPC4^{-/-} mice.

Impaired Ca^{2+} Influx in TRPC4^{-/-} Endothelial Cells in Response to Thrombin

We measured the thrombin-induced rise in intracellular Ca^{2+} ($[\text{Ca}^{2+}]_i$) in mouse LECs isolated from wt or TRPC4^{-/-} mice. Fura 2-loaded wt LECs were challenged with either thrombin (5 U/mL) or the PAR-1-specific agonist peptide ($5 \mu\text{mol/L}$).

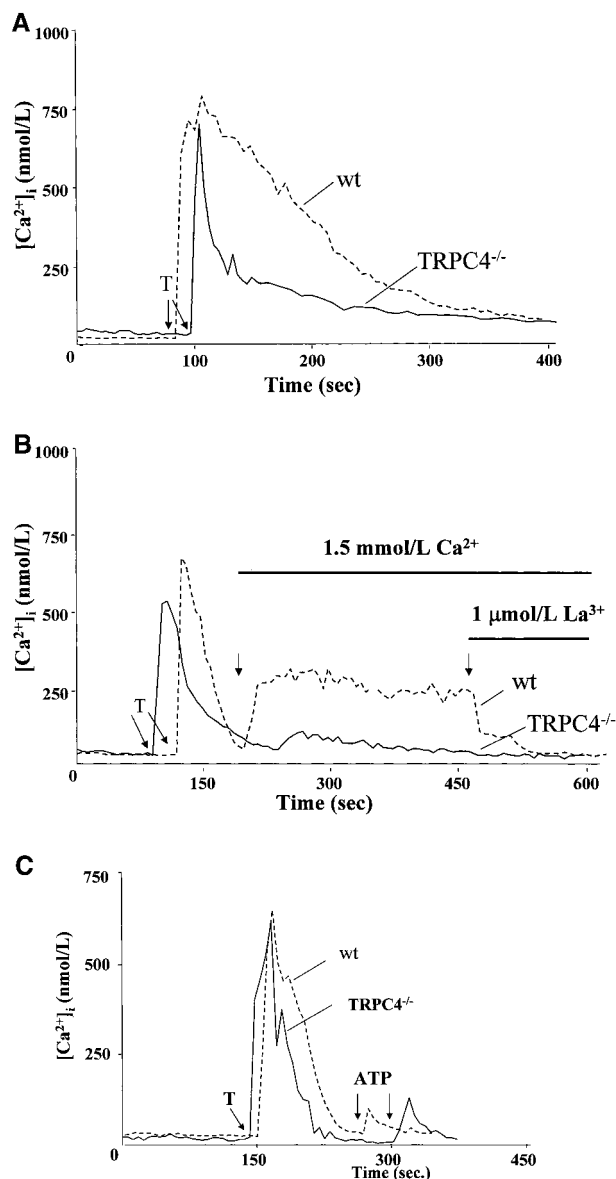


Figure 2. A, Effects of thrombin on $[Ca^{2+}]_i$ in LECs. Thrombin-induced increase in $[Ca^{2+}]_i$ was measured as described in Materials and Methods. In each experiment, 25 to 35 cells were selected to measure changes in $[Ca^{2+}]_i$. Extracellular Ca^{2+} concentration was 1.26 mmol/L. Arrows signify time thrombin (5 U/mL) was added. Results are representative of 4 experiments and are summarized in Table 1. T indicates thrombin. B, TRPC4^{-/-} LECs fail to show thrombin-induced Ca^{2+} influx. Thrombin-induced Ca^{2+} influx was measured in wt and TRPC4^{-/-} LECs. Fura 2-AM loaded cells were washed 2 times, placed in Ca^{2+} - and Mg^{2+} -free HBSS, and then stimulated with thrombin (5 U/mL). After return of $[Ca^{2+}]_i$ to baseline levels, cells were stimulated with $CaCl_2$ (1.5 mmol/L) and at the indicated time lanthanum chloride (1 μ mol/L) was added to inhibit Ca^{2+} influx. The experiment was repeated 3 times with similar results. C, Effects of thrombin on Ca^{2+} store depletion. Cells were first stimulated with thrombin (5 U/mL) in the absence of extracellular Ca^{2+} . After recovery to the baseline value, cells were challenged with ATP (5 μ mol/L). Note that there was no significant increase in $[Ca^{2+}]_i$ in response to ATP. Experiment was repeated 3 times with similar results.

In the presence of extracellular Ca^{2+} (1.26 mmol/L), thrombin produced an increase in $[Ca^{2+}]_i$ (peak value 750 ± 55 nmol/L) followed by a gradual decline to baseline value (Figure 2A). PAR-1 agonist peptide produced a similar response in wt

TABLE 1. Inhibition of PAR-1 Activation-Induced Increase of $[Ca^{2+}]_i$ in TRPC4^{-/-} LECs

Condition	3-Minute Area in TRPC4 ^{-/-} (% decrease of wt value)
Thrombin (5 U/mL)	$55 \pm 4.6^*$
TFLLRNPNNDK-NH ₂ (5 μ mol/L)	$56 \pm 5.2^*$

Values are mean \pm SE from 3 to 4 experiments.

Endothelial cells grown on glass coverslips were loaded with fura 2-AM and then challenged with either thrombin or TFLLRNPNNDK-NH₂ (PAR-1-specific agonist peptide) in the presence of extracellular Ca^{2+} (1.26 mmol/L).

In each experiment, 25 to 35 cells were selected to measure the change in $[Ca^{2+}]_i$. Ca^{2+} transient for a period of 3 minutes after agonist stimulation was integrated to obtain the area. Relative area in wt LECs was considered as 100% to compare with TRPC4^{-/-} LECs. Other details are described in Materials and Methods. Original recordings in the Ca^{2+} transient are given in Figure 2A. *Decrease in area from wt LECs, $P < 0.05$.

LECs (Table 1). In TRPC4^{-/-} LECs, thrombin-induced increase in initial peak $[Ca^{2+}]_i$ was similar to wt LECs, but the sustained phase was considerably reduced in TRPC4^{-/-} (Figure 2A and Table 1). We compared the increase in $[Ca^{2+}]_i$ in wt and TRPC4^{-/-} mice LECs by integrating the area under the Ca^{2+} transient for a 3-minute period after exposure to thrombin or PAR-1 agonist peptide. We observed a $\approx 55\%$ reduction in the increase in $[Ca^{2+}]_i$ in TRPC4^{-/-} LECs compared with wt LECs (Figure 2A and Table 1), regardless of the agonist used.

To further discriminate between increase of $[Ca^{2+}]_i$ due to Ca^{2+} release from internal stores or Ca^{2+} entry, we first depleted the endoplasmic Ca^{2+} store with thrombin in the absence of extracellular Ca^{2+} , and we then reapplied Ca^{2+} to assess Ca^{2+} influx through the channels. In this experiment, thrombin produced a similar increase in peak $[Ca^{2+}]_i$ in both wt and TRPC4^{-/-} cells (Figure 2B). In wt, replenishing Ca^{2+} (1.5 mmol/L) in the extracellular medium after store depletion caused a prolonged Ca^{2+} influx, which was completely blocked by the addition of La^{3+} (1 μ mol/L) (Figure 2B). In contrast to wt cells, replenishing extracellular Ca^{2+} after store depletion with thrombin caused almost no significant Ca^{2+} influx in TRPC4^{-/-} LECs (Figure 2B). We compared the thrombin-induced Ca^{2+} influx between these two cell types by integrating the area over 4 minutes after Ca^{2+} reapplication. We observed a 75% to 80% reduction in Ca^{2+} influx in TRPC4^{-/-} LECs compared with wt LECs.

To address whether the reduced Ca^{2+} influx in TRPC4^{-/-} LECs was not secondary to an incomplete Ca^{2+} store depletion induced by thrombin, we measured the effects of ATP after challenging these cells with thrombin in the absence of extracellular Ca^{2+} (Figure 2C). In these experiments, cells were first challenged with thrombin, and after recovery to the baseline, the cells were challenged with ATP. Addition of ATP did not significantly increase $[Ca^{2+}]_i$ in either wt or TRPC4^{-/-} mice LECs, suggesting that thrombin addition had depleted the stores. We also confirmed that ATP is as potent an agonist as thrombin in depleting the intracellular Ca^{2+} stores in LECs obtained from wt and TRPC4^{-/-} endothelial cells (data not shown).

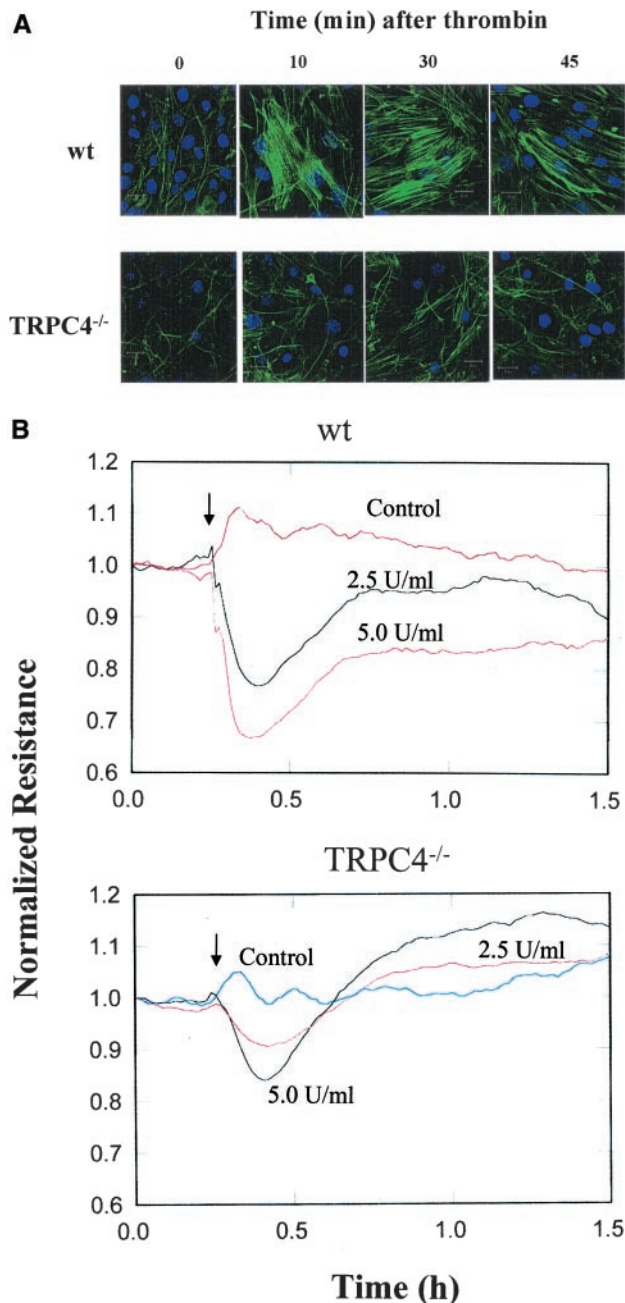


Figure 3. A, Lack of thrombin-induced actin stress fiber formation in TRPC4^{-/-} mice LECs. LECs were grown to confluence on gelatin-coated glass coverslips. Cells were stimulated with 5 U/mL thrombin for the indicated time intervals. Cells were then washed, fixed, and stained with Alexa-488 phalloidin to detect actin polymerization and DAPI to visualize the nucleus as described in Materials and Methods. Results are representative of 3 experiments. Bar=20 μ m. B, Effects of thrombin on wt and TRPC4^{-/-} LEC transendothelial monolayer electrical resistance values. LECs were grown to confluence on gold electrodes (see Materials and Methods). Before the experiments, cells were washed twice and incubated with 1% FBS containing growth medium for 2 hours before the addition of thrombin. Arrow indicates the time thrombin was added. Experiment shown is representative of 4 trials.

Prevention of Thrombin-Induced Stress Fiber Formation in TRPC4^{-/-} Endothelial Cells

To address whether thrombin-induced Ca²⁺ influx through TRPC4 channel mediates cytoskeletal reorganization, we

TABLE 2. Effects of Thrombin on Transendothelial Monolayer Electrical Resistance

Condition	Percent Maximum Decrease in Normalized Resistance	
	wt LECs	TRPC4 ^{-/-} LECs
Thrombin (2.5 U/mL)	23 \pm 2	10 \pm 1*
Thrombin (5.0 U/mL)	35 \pm 3	16 \pm 1*

LEC monolayer electrical resistance was measured as described in Materials and Methods. Maximum thrombin-induced decrease in monolayer resistance was expressed as a percentage decrease of basal value. Values shown are mean \pm SEM from 4 experiments. *Difference from wt LECs, $P<0.05$.

measured actin-stress fiber formation both in wt and TRPC4^{-/-} LECs (Figure 3A). Exposure of thrombin caused actin-stress fiber formation in wt but not in TRPC4^{-/-} LECs (Figure 3A). We observed a characteristic pattern of peripheral actin staining in TRPC4^{-/-} LECs (Figure 3A).

Impaired Thrombin-Induced Endothelial Cell Retraction in TRPC4^{-/-} Endothelial Cells

Because store depletion-activated Ca²⁺ influx and actin-stress fiber formation were prevented in TRPC4^{-/-} LECs, we measured thrombin-induced changes in transendothelial monolayer electrical resistance to assess endothelial cell retraction (ie, cell shape change), a prerequisite for the increase in endothelial permeability.^{20,21} Thrombin exposure to wt LEC monolayer produced a maximum decrease in transendothelial monolayer electrical resistance of \approx 35%, and the value returned to normal 1 hour after thrombin challenge (Figure 3B and Table 2). By contrast, exposure of thrombin to TRPC4^{-/-} LECs produced only a \approx 16% decrease and the decrease in resistance returned to baseline within only 20 minutes after thrombin (Figure 3B and Table 2).

Reduction in Thrombin-Induced Increase in Lung Vascular Permeability in TRPC4^{-/-} Mice

We measured microvessel liquid permeability in isolated lung preparations from wt and TRPC4^{-/-} mice. Basal values of $K_{f,c}$ did not significantly differ between wt and TRPC4^{-/-} lungs (mean \pm SD; n=5 to 6; $7\times 10^{-3}\pm 0.4\times 10^{-3}$ versus $6.3\pm 0.6\times 10^{-3}$ mL/min per cm H₂O/g). In wt mice, PAR-1 agonist peptide (5 μ mol/L) produced a 3-fold increase in lung $K_{f,c}$ within 15 minutes (Figure 4). The factor of increase was only 1.5-fold in lungs from TRPC4^{-/-} mice (Figure 4). After a 15-minute washout period to remove PAR-1 agonist, the changes in permeability were reversed both in wt and TRPC4^{-/-} mice (Figure 4). Because we showed that La³⁺ (1 μ mol/L) inhibited thrombin-induced Ca²⁺ influx, we predicted that La³⁺ should reduce PAR-1-mediated changes in vascular permeability in wt lung preparations to the same extent as deletion of TRPC4 gene. This was indeed the case because in wt mice the PAR-1 agonist peptide (5 μ mol/L) produced only a 1.4-fold increase of $K_{f,c}$ in the presence of 1 μ mol/L La³⁺ (see Figure 4).

Discussion

Activation of nonexcitable cells with G_q-linked receptor agonists results in release of Ca²⁺ from intracellular stores

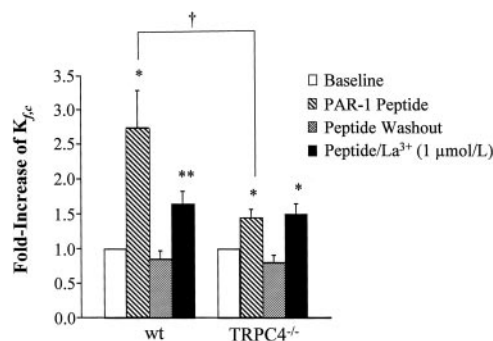


Figure 4. Genetic and pharmacological inhibition of the effects of PAR-1 agonist peptide (5 $\mu\text{mol/L}$) in increasing microvessel permeability in mouse lung preparation. Factor of increase in microvascular permeability ($K_{f,c}$) is plotted for wt and TRPC4^{-/-} groups. In wt lung preparations, note the greater effect of peptide above basal level (1.0) and marked inhibitory effect of La³⁺ (1 $\mu\text{mol/L}$). Error bars, SD; n=5 to 6 in each group. *Different from baseline value ($P<0.05$); **Inhibitory effect of La³⁺ ($P<0.05$); †Reduced response of TRPC4^{-/-} for PAR-1 agonist peptide compared with wt ($P<0.05$).

followed by a transmembrane Ca²⁺ influx.^{9,10,12–14} The Ca²⁺ influx accounts for the second phase of the increased [Ca²⁺]_i.^{9,10,12–14} In endothelial cells, the sustained Ca²⁺ influx from the extracellular medium contributes to the increase of the cytosolic Ca²⁺ concentration, which is necessary for the release of vasoactive substances such as nitric oxide or prostaglandins,^{9,10} and may be involved in the mechanism of increased endothelial permeability.^{4,5,7,14} Several members of the mammalian TRPC gene family channels have been shown to function as store-operated cation channels,^{9,10,12–14} and these channels are expressed in endothelial cells.^{9,10,15,16} Freichel et al¹⁷ have recently developed TRPC4 knockout (TRPC4^{-/-}) mice and investigated store-operated Ca²⁺ current and Ca²⁺ entry in aortic endothelial cells (AECs). In TRPC4^{-/-} AECs, IP₃/BHQ-activated SOC current was absent, and also the acetylcholine-induced endothelium-dependent vasorelaxation was reduced compared with wt.¹⁷

In the present study, we showed that TRPC4 mRNA transcript was absent in TRPC4^{-/-} mouse LECs, whereas marked expression was evident in wt LECs. Disruption of the TRPC4 gene in mice did not alter the expression profile of the other predominant TRPC isoforms in LECs (TRPC1, TRPC3, and TRPC6). We showed that thrombin produced a prolonged increase of the [Ca²⁺]_i in wt LECs compared with the TRPC4^{-/-} LECs. Further, Ca²⁺ entry after thrombin-induced Ca²⁺ store depletion caused a prolonged Ca²⁺ influx, which was inhibited by 1 $\mu\text{mol/L}$ La³⁺ in wt LECs. In contrast, thrombin-induced Ca²⁺ influx was nearly absent in TRPC4^{-/-} LECs. Previous studies showed that TRPC4 is highly specific in mediating Ca²⁺ entry in mouse endothelial cells.¹⁷ Our results demonstrate that TRPC4 is also essential for thrombin-induced Ca²⁺ entry.

We addressed whether the rise in [Ca²⁺]_i secondary to activation of TRPC4 is involved in the mechanism of actin cytoskeletal reorganization in endothelial cells induced by thrombin.^{20,21} In wt LECs, we observed thrombin-induced actin stress fiber formation, and this was absent in TRPC4^{-/-}

LECs. These results show that TRPC4 activation-mediated Ca²⁺ influx is a critical determinant of the thrombin-induced cytoskeletal reorganization in mouse LECs. As a functional measure of cytoskeletal reorganization-dependent interendothelial gap formation, we quantified transendothelial electrical resistance in confluent monolayers of mouse endothelium. The results showed that cytoskeletal reorganization is necessary for gap formation (and hence increased endothelial permeability), because the cells from TRPC4^{-/-} mice showed a smaller change in their transendothelial electrical resistance in response to thrombin.

We also investigated the possible role of TRPC4 channel activation in the thrombin-induced increase in the microvascular permeability in the intact lung (ie, by measurement of $K_{f,c}$). By comparing PAR-1 mediated increase of $K_{f,c}$ in wt and TRPC4^{-/-}, we showed that TRPC4 expression is required for a substantial component of the increase in microvessel permeability in intact lungs. Thus, in the TRPC4^{-/-} group, the agonist-induced permeability was reduced from wt value of ≈ 3.0 to 1.5. The involvement of TRPC4 channels in PAR-1-mediated permeability changes was supported by our finding of a marked inhibitory effect of La³⁺ (1 $\mu\text{mol/L}$) in wt lung preparations. The residual effect of agonist peptide seen in the TRPC4 knockout mice probably reflects the fact that agonists can still produce a rise in [Ca²⁺]_i via other ion channels, albeit the response was attenuated and briefer owing to the lack of competent TRPC4 channels.

Our results suggest the following sequence of events mediating increase in lung vascular permeability after PAR-1 activation: (1) G_q-linked PLC activation and increase in IP₃; (2) intracellular Ca²⁺ store depletion and Ca²⁺ influx determined by TRPC4; and (3) Ca²⁺-dependent cytoskeletal reorganization and interendothelial gap formation.

Acknowledgments

This work was supported by the National Institute of Health grants GM-58531, HL-45638, T32-HL-077829, and in part by Deutsche Forschungsgemeinschaft and Fonds der Chemischen Industrie.

References

- Lum H, Malik AB. Regulation of vascular endothelial barrier function. *Am J Physiol Lung Cell Mol Physiol.* 1994;267:L223–L241.
- Malik AB, Fenton JW II. Thrombin-mediated increase in vascular endothelial permeability. *Sem Throm Hemost.* 1992;18:193–199.
- Vogel SM, Gao X, Mehta D, Ye RD, John TA, Andrade-Gordon P, Tirupathi C, Malik AB. Abrogation of thrombin-induced increase in pulmonary microvascular permeability in PAR-1 knockout mice. *Physiol Genomics.* 2000;4:137–145.
- Sandoval R, Malik AB, Naqvi T, Mehta D, Tirupathi C. Requirement for Ca²⁺ signaling in the mechanism of thrombin-induced increase in endothelial permeability. *Am J Physiol Lung Cell Mol Physiol.* 2001;280:L239–L247.
- Sandoval R, Malik AB, Minshall RD, Kouklis P, Ellis CA, Tirupathi C. Ca²⁺ signaling and PKC α activate increased endothelial permeability by disassembly of VE-cadherin junctions. *J Physiol.* 2001;533:433–445.
- Ellis CA, Tirupathi C, Sandoval R, Niles WD, Malik AB. Time course of recovery of endothelial cell surface thrombin receptor (PAR-1) expression. *Am J Physiol Cell Physiol.* 1999;276:C38–C45.
- Lum H, Aschner JL, Phillips PG, Fletcher PW, Malik AB. Time-course of thrombin-induced increase in endothelial permeability: relationship to [Ca²⁺]_i and inositol polyphosphates. *Am J Physiol Lung Cell Mol Physiol.* 1992;263:L219–L225.
- Tirupathi C, Naqvi T, Sandoval R, Mehta D, Malik AB. Synergistic effects of tumor necrosis factor- α and thrombin in increasing endothelial

- permeability. *Am J Physiol Lung Cell Mol Physiol*. 2001;281:L958–L968.
9. Nilius B, Droogmans G. Ion channels and their role in vascular endothelium. *Physiol Rev*. 2001;81:1415–1459.
 10. Freichel M, Schweig U, Stauffberger S, Freise D, Schorb W, Flockerzi V. Store-operated cation channels in the heart and cells of the cardiovascular system. *Cell Physiol Biochem*. 1999;9:270–283.
 11. Montell C, Birnbaumer L, Flockerzi V. The TRP channels: a remarkable functional family. *Cell*. 2002;108:595–598.
 12. Boulay G, Zhu X, Peyton M, Jiang M, Hurst R, Stefani E, Birnbaumer L. Cloning and expression of a novel mammalian homolog of *Drosophila* Transient Receptor Potential (Trp) involved in calcium entry secondary to activation of receptors coupled by the G_q class of G proteins. *J Biol Chem*. 1997;272:29672–29680.
 13. Liu X, Wang W, Sing BB, Lockwich T, Jadowiec J, O'Connell B, Wellner R, Zhu MX, Ambudkar IS. Trp1, a candidate protein for the store-operated Ca²⁺ influx mechanism in salivary gland cells. *J Biol Chem*. 2000;275:3403–3411.
 14. Putney JW Jr. TRP, inositol 1, 4, 5-trisphosphate receptors, and capacitative calcium entry. *Proc Natl Acad Sci U S A*. 1999;96:14669–14671.
 15. Moore TM, Brough GH, Babal P, Kelley JJ, Li M, Stevens T. Store-operated calcium entry promotes shape change in pulmonary endothelial cells expressing Trp1. *Am J Physiol Lung Cell Mol Physiol*. 1998;275:L574–L582.
 16. Brough GH, Wu S, Cioffi D, Moore TM, Li M, Dean N, Stevens T. Contribution of endogenously expressed Trp1 to a Ca²⁺-selective, store-operated Ca²⁺ entry pathway. *FASEB J*. 2001;15:1727–1738.
 17. Freichel M, Suh SH, Pfeifer A, Schweig U, Trost C, Weißgerber P, Biel M, Philipp S, Freise D, Droogmans G, Hofmann F, Flockerzi V, Nilius B. Lack of an endothelial store-operated Ca²⁺ current impairs agonist-dependent vasorelaxation in TRP4^{-/-} mice. *Nat Cell Biol*. 2001;3:121–127.
 18. Tiruppathi C, Yan W, Sandoval R, Naqvi T, Pronin AN, Benovic JL, Malik AB. G protein-coupled receptor kinase-5 regulates thrombin-activated signaling in endothelial cells. *Proc Natl Acad Sci U S A*. 2000;97:7440–7445.
 19. Tiruppathi C, Malik AB, Del Vecchio PJ, Keese CR, Giaever I. Electrical method for detection of endothelial cell shape change in real time: assessment of endothelial barrier function. *Proc Natl Acad Sci U S A*. 1992;89:7919–7923.
 20. Garcia JG, Davis HW, Patterson CE. Regulation of endothelial gap formation and barrier dysfunction: role of myosin light chain phosphorylation. *J Cell Physiol*. 1995;163:510–522.
 21. Goeckeler ZM, Wysolmerski RB. Myosin light chain kinase-regulated endothelial cell contraction: the relationship between isometric tension, actin polymerization, and myosin phosphorylation. *J Cell Biol*. 1995;130:613–627.